Journal of Nuclear Materials 390–391 (2009) 156–159

Contents lists available at ScienceDirect

Journal of Nuclear Materials

journal homepage: www.elsevier.com/locate/jnucmat

Micro/nano scale modification of plasma facing components in LHD and its impact on the metal dust generations

M. Tokitani [a,*], Y. Ohtawa [b], N. Yoshida [b], K. Tokunaga [b], T. Fujiwara [b], N. Ashikawa [a], S. Masuzaki [a], H. Yamada [a], A. Sagara [a], N. Noda [a], A. Komori [a], LHD experimental group [a]

[a] National Institute for Fusion Science, 322-6 Oroshi, Toki, Gifu 509-5292, Japan
[b] Research Institute for Applied Mechanics, Kyushu University, Kasuga, Fukuoka 816-8580, Japan

ARTICLE INFO

PACS:
28.52.−s
28.52.Fa
52.40.Hf
52.55.Hc
61.72.Qq

ABSTRACT

First walls and divertor plates of large helical device (LHD) are made of stainless steels and isotropic graphite, respectively. They are bombarded by energetic plasma particles, and are caused the radiation damages. For understanding of long term irradiation effects of metallic first walls, probe specimens of Mo were mounted on the special sample stage of outer-port of the LHD torus which is located at about 2500 mm from LCFS (last closed flux surface) of heliotron plasma, and then, exposed to plasma discharges through the single experimental campaign. Majority of discharge gas was hydrogen or helium. Amorphous re-deposition layer of about few nm thick and large sized blisters with few micrometer were formed at the specimen surface. Formation of dense gas bubbles (1–2 nm), dislocation loops and surface roughening were simultaneously occurred in the sub-surface layer about 30 nm thick. Such nano scale damages may be mainly caused by helium particle bombardment.

1. Introduction

Large helical device (LHD) is the world's largest heliotron-type plasma machine equipped with superconducting magnetic coil system [1]. LHD has large advantage for current-less disruption-free steady state plasma operations [2]. A high-temperature and long-pulse plasma was created and maintained for 54 min with 1.6 GJ in the 2005FY experimental campaign with employing the magnetic axis sweeping to disperse the plasma heat load. However, the plasma collapse was frequently observed at the end of the long-pulse plasma operation because of metal flakes dropping into the plasma from the wall or divertor plates [3].

First walls and divertor plates of LHD are made of stainless steels (SUS316L) and isotropic graphite (IG-430U), respectively. The former is the major material in LHD, and the graphite area is only about 5% of the total plasma facing area. They are frequently exposed to not only main plasma discharges but also many type of wall conditioning processes such as glow discharge cleanings (GDCs), Ti gettering and boronizations. Thus, surface conditions of plasma facing components (PFCs) are different with places. In addition to radiation damages, mix-material re-deposition layer composed by Fe, Cr, C and O are formed on PFCs [4,5]. If such deposition layers were emitted from the surfaces, they may act as the effective metal impurities (so-called dust) for plasma. Undesired metal flake penetration to the plasma mentioned above must be closely related of them. Therefore, change of the microscopic characteristics of PFCs is important for steady state plasma operations.

To clarify the microscopic modification of first walls after exposed to LHD plasmas, material probe experiment through the single experimental campaign was conducted.

2. Experimental procedures

Pre-thinned and electro-polished Mo discs of 3 mm diameter for TEM observation and bulk Mo plates of 0.1 mm thickness were prepared for probe specimen. They were mounted on the special sample stage of outer-port of the LHD torus which is located at about 2500 mm from LCFS (last closed flux surface) of heliotron configuration as shown in Fig. 1, and then, exposed to the plasma discharges through the 2006FY experimental campaign. Table 1 shows total shot and discharge time for each discharge type during 2006FY campaign. Upper three series are main plasma discharges with helical magnetic field, and lower four series are glow discharge cleanings (GDCs) without magnetic fields. The sample stage makes possible to select desirable plasma discharges by using rotatable shutter mechanism. Three types of exposure were selected in this experiment: (1) only main plasma discharges, and (2) only GDCs, (1) + (2): both main plasma and GDCs. Ion current and voltage to the whole first wall on GDCs is about 20 A and 200 V, respectively. Thus, the total fluence through this campaign were roughly estimated to be 1.5×10^{23} H/m^2, 2.4×10^{23} He/m^2,

* Corresponding author. Tel.: +81 572 58 2143; fax: +81 572 58 2618.
E-mail address: tokitani.masayuki@LHD.nifs.ac.jp (M. Tokitani).

0022-3115/$ - see front matter © 2009 Elsevier B.V. All rights reserved.
doi:10.1016/j.jnucmat.2009.01.156

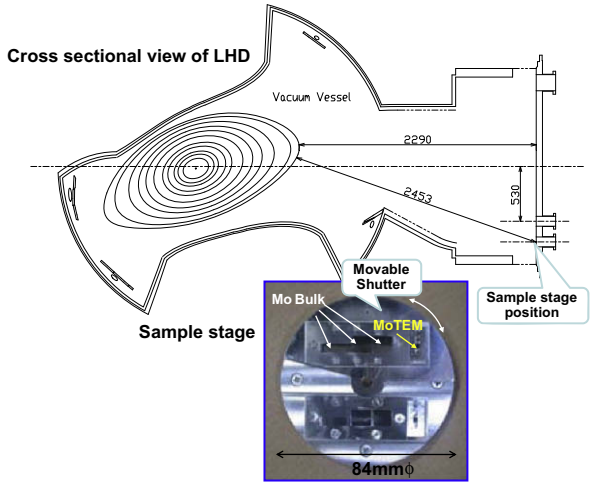

Fig. 1. Schematic view of the experimental set up in LHD.

Table 1
Total shot and discharge time for each discharge type during 2006 campaign.

Exposure case		Discharge type	Total shot	Total discharge time (h)
(1) + (2)	(1)	H plasma	4531 shot	
		He plasma	1601 shot	
		Ne, Xe plasma	233 shot	
	(2)	H-GDC	18 shot	265.8
		He-GDC	41 shot	418.2
		Ne-GDC	4 shot	61.7
		Ar-GDC	3 shot	17.4

respectively. In the case of main plasma discharges, main component of incidence particles to the specimens is charge-exchanged neutrals (CX-neutrals) with the energy of ~1 keV. From our previous study, incidence flux and energy of CX-neutrals to the first wall during main plasma discharge was estimated to be $\sim 1 \times 10^{19}$ ions/m^2s and ~1 keV, respectively [6]. If the average discharges time was assumed to be 2 s, total fluence on this experiment is roughly estimated to be about 9.0×10^{22} H/m^2, 3.2×10^{22} He/m^2, respectively. This may be very rough and overestimated value, because specimens were located very far from the first wall position. However, it is important for discussion on this study.

After the exposure, surface modification and microscopic damage were analyzed by means of transmission electron microscopy (TEM), scanning electron microscopy (SEM) and atomic force microscopy (AFM). The focused ion beam (FIB) technique was used to fabricate a cross-sectional thin TEM sample.

Furthermore, to investigate the effects of plasma exposure on optical reflectivity of Mo mirror, change of optical reflectivity was measured by means of spectrophotometer for the wave length of 190–2500 nm. Since optical reflectivity is strongly influenced by radiation damages on the surface [7], measurement of it is important for not only evaluation of the optical characteristics but also the radiation damages.

3. Results and discussion

3.1. Surface modification

Fig. 2 shows SEM and AFM images of Mo after exposed to the case of (1), (2) and (1) + (2). The upper series of micrograph shows that in the case of (2) and (1) + (2), large blisters with size of over 20 μm in diameter and the dusts with size of few micrometer were formed on the surface. The number of them is more remarkable at

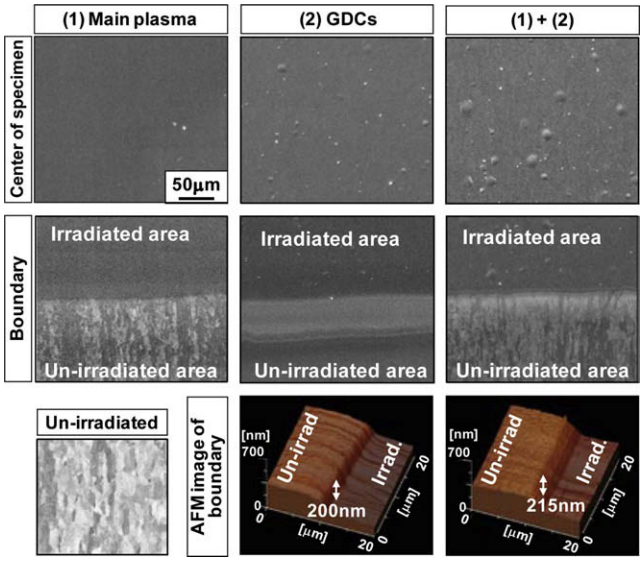

Fig. 2. Upper series; SEM images of exposed specimen. Middle series; SEM images of boundary between exposed and un-exposed area. Lower series; AFM images of boundary area.

the case of (1) + (2). The middle series shows boundary between exposed and un-exposed area. In all cases, the surface condition after irradiation has changed. And also, the lower series shows AFM images of boundary area. It was clear that exposed area of (2) and (1) + (2) suffered strong sputtering erosion over 200 nm. In contrast, exposed area of (1), some erosion was observed, but intensive deformation such as blisters and dusts were not identified. The results indicate that GDCs has a major role for surface modification and sputtering erosion than that of main plasma discharges.

Fig. 3 shows a cross-sectional TEM image of large blister at the case of (1) + (2) fabricated by FIB technique. Strong black layer of top surface with ~0.5 μm thick is protection layer for FIB fabrication. Grains with different orientation are shown by different contrast. It should be noted that thickness of the blister's lid was estimated at about 2 μm, and fracture and upheaval of it has been occurring from grain boundaries. It is considered that injected hydrogen atoms during main plasma discharges and GDCs were diffused up to 2 μm, and were accumulated in grain boundary which may act as effective trapping site of hydrogen atoms. Newly, injected hydrogen atoms were continuously trapped along the grain boundary one after another, and formed the highly pressurized and expanding fields on grain boundaries. Finally, they caused intergranular fractures. In the case of helium ion irradiation in metals up to the dose of $\sim 10^{23}$ He/m^2 with low energy (<1 keV), such a large size blisters will not be formed [8,9]. Because helium once injected in metals with low energies (<1 keV) is immediately trapped by lattice defects which exist in the project range of it (10–

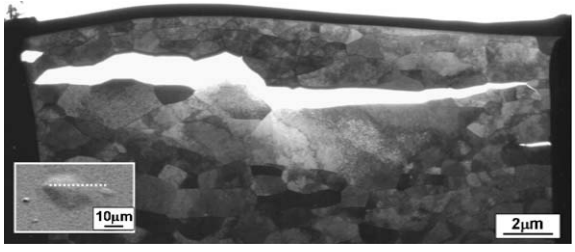

Fig. 3. Cross-sectional TEM image of large blister at the case of (1) + (2) fabricated by FIB technique.

20 nm). Therefore, they cannot diffuse up to the depth of 2 μm. Details are discussed in Section 3.2.

3.2. Microscopic damage and impurity deposition

Fig. 4 shows TEM images with electron diffraction pattern of Mo exposed to (1), (2) and (1) + (2). The upper series of micrographs are bright field images with large deviation parameter *s* (deviation from the Bragg condition [10]). White dot images are gas bubbles. The lower series are dark field images with small deviation parameter *s*, which fits for observation of defects with strong lattice distortion such as dislocation loops. Considerably large amounts of bubbles and dislocation loops were formed in all cases. They may have been caused by helium irradiations, because it is known that injected helium in metals causes intensive radiation damages due to the strong interaction with lattice defects such as vacancies and dislocations [11]. In contrast, hydrogen irradiation cases, such damages are scarcely formed even at a high dose level. In addition to the diffraction spots from the Mo, halo diffraction rings of (2) and (1) + (2) indicate that amorphous like re-deposition layer with few nm thick was formed on the surface. From our previous study, it is clear that first wall components of Fe and Cr were deposited during GDCs even if at sputtering dominant condition [12]. Therefore, the surface of them has been becoming a very complex structure composed by deposits (e.g. Fe and Cr) and radiation damages.

In order to know depth distribution of internal damage, cross-sectional TEM observations were also performed for three exposure cases. The results are shown in Fig. 5. In the case of (1) + (2), very heavy damages such as dense bubbles with size of 1–2 nm and surface roughening were simultaneously occurred in the sub-surface region about 30 nm thick. In contrast, for the case of (1), although small bubbles were observed in about 30–40 nm thick, size and density of them were not so remarkable than that of (2) and (1) + (2). In the case of (2), small bubbles with size of 1–2 nm were observed with high density on sub-surface layer about 10 nm thick which may be mainly caused by helium GDC [12]. Probably, the injected helium atoms were not able to pass this layer. As mentioned in Section 3.1, almost all the injected helium atoms must be trapped within the projection range. The result of (2) is supported by this explanation.

According to the other researches [13,14], although estimated total fluence of hydrogen in the case of (2) and (1) + (2) was much lower than that of critical fluence of blister formation, large size blisters were clearly confirmed. The possible formation mechanism was proposed as following. Helium bubbles and dislocation loops near the surface were made strong stress field around them, and the bubbles and stress fields may be able to act as the diffusion barrier for hydrogen atoms. Particularly, high energy hydrogen

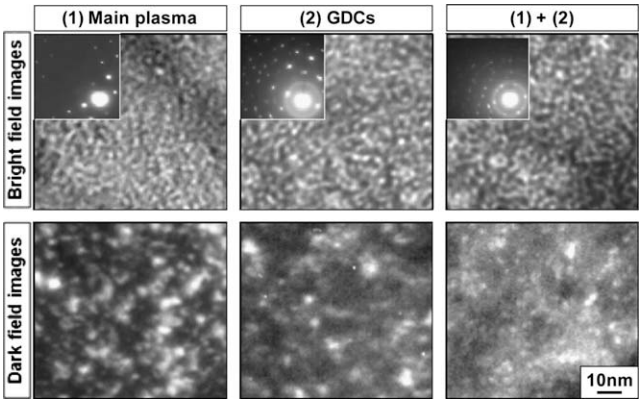

Fig. 4. TEM images with electron diffraction pattern of Mo after exposed to the case of (1), (2) and (1) + (2) in Table 1.

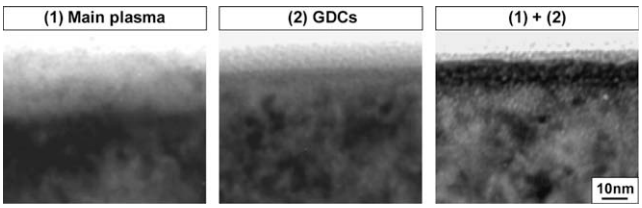

Fig. 5. Cross-sectional TEM images of three exposure cases in Table 1.

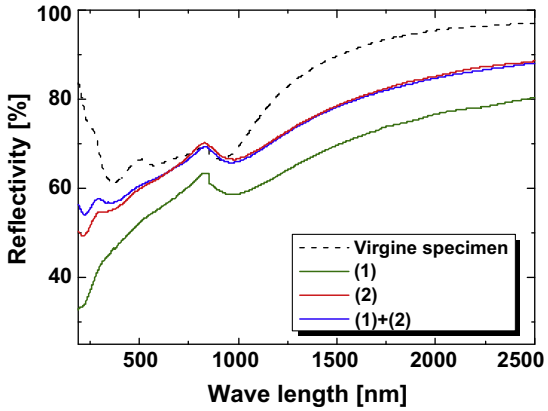

Fig. 6. Optical reflectivity of Mo after exposed to three exposure cases in Table 1.

e.g. CX-neutrals, has longer range than the thickness of strong damaging layer mainly caused by helium GDC, and they can be retained effectively. Thus, the injected hydrogen atoms were difficult to be released from the surface, and were accumulated in grain boundaries, and finally, they formed large size blisters. For exact discussions, further fundamental studies will be required in future.

The present results indicate that formation of bubbles and blisters must be lead to the undesired impurity generations in LHD even at the bottom port of the torus.

3.3. Change of optical reflectivity

Fig. 6 shows the optical reflectivity of Mo specimen after exposed to three exposure cases by using spectrophotometer. Reflectivity of virgin specimen was also plotted together. It is clear that reduction of reflectivity has occurred in all cases, and it near 200 nm or less and also infrared region was remarkable. The spectrum of (1) which was exposed to only main plasma discharges is significantly large reduction. Although we cannot explain this phenomenon well now, it seems to be due to the energetic neutral-helium bombardment with the energy of ~1 keV which was created by charge-exchange collisions. It was reported that effects of helium bombardment are three orders of magnitude higher than that of hydrogen bombardment for optical reflectivity [7]. In that case, it is considered that reduction of optical reflectivity is due to the multiple scattering of light by the helium bubbles in the sub-surface region. It should be noted that specimens were placed to bottom of the outer-port, where relatively far from the first wall position (see Fig. 1). In future fusion devices, mirrors for plasma diagnosis will be designed at same manners. In that case, reduction of reflectivity due to the plasma bombardment is serious problem.

4. Summary

Understanding of the irradiation effects of metallic first walls during single experimental campaign, material probe experiments

were conducted. After the exposure, amorphous re-deposition layer of about few nm thick composed of deposited impurities were formed on the specimen surface. Formation of dense gas bubbles (1–2 nm), dislocation loops and surface roughening were simultaneously occurred in the sub-surface layer about 30 nm thick. Such damage may be mainly caused by helium particle bombardment [12]. Furthermore, large blisters with size of over 20 μm in diameter were observed. From the cross-sectional TEM observation, thickness of the blister's lid was estimated at about 2 μm, and it had been fracturing at the grain boundaries. It could be caused by the injected hydrogen atoms, because almost all the injected helium atoms were easily trapped at up to about 30 nm from the surface (see Fig. 5), and they may have been difficult to diffuse up to 2 μm. The present results indicate that formation of bubbles and blisters must be lead to the undesired impurity generations in LHD even at the bottom port of the torus.

Optical reflectivity of Mo after exposed to three exposure cases was measured by spectrophotometer. Reduction of reflectivity has occurred in all cases, and it near 400 nm or less was especially remarkable. It should be noted that these specimens were placed to relatively far from the first wall position. In future fusion devices, mirrors for plasma diagnosis will be designed at same manners. In that case, present study indicates that reduction of reflectivity due to the plasma bombardment is serious problem.

The technique of this research with TEM observation is very useful for PWI studies on not only LHD but also future fusion devices.

References

[1] O. Motojima et al., Nucl. Fus. 43 (2003) 1674.
[2] A. Sagara et al., J. Nucl. Mater. 313–316 (2003) 1.
[3] T. Mutoh et al., Nucl. Fus. 47 (2007) 1250.
[4] Y. Nobuta et al., Fus. Eng. Des. 81 (2006) 187.
[5] T. Hino et al., Fus. Eng. Des. 82 (2007) 1621.
[6] M. Tokitani et al., J. Nucl. Mater. (accepted for publication).
[7] A. Ebihara et al., J. Nucl. Mater. 363–365 (2007) 1195.
[8] D. Nishijima et al., J. Nucl. Mater. 313–316 (2003) 97.
[9] D. Nishijima et al., J. Nucl. Mater. 329–333 (2004) 1029.
[10] M. Kiritani et al., J. Nucl. Mater. 251 (1997) 237.
[11] M. Tokitani et al., J. Nucl. Mater. 329–333 (2004) 761.
[12] M. Tokitani et al., Nucl. Fus. 45 (2005) 1544.
[13] M.Y. Ye et al., J. Nucl. Mater. 313–316 (2003) 72.
[14] T. Venhaus et al., J. Nucl. Mater. 290–293 (2001) 505.